

On a spectral solver for highly oscillatory and non-smooth solutions of a class of linear fractional differential systems

Amin Faghih^{1a}

¹*Department of Computer Science, KU Leuven, Leuven, Belgium*
^a*amin.faghih@kuleuven.be*

November 11, 2025

Abstract

This study discusses a class of linear systems of fractional differential equations with non-constant coefficients, with a particular focus on problems exhibiting highly oscillatory and non-smooth behavior. We first establish the regularity properties of the solutions under specific conditions on the input data. A spectral Galerkin method based on Müntz-Jacobi functions is developed that efficiently handle the non-smooth and highly oscillatory solutions. A key advantage of the proposed approach is the ability to compute the approximate solution via recurrence relations, avoiding the need to solve complex algebraic systems. Moreover, the method remains stable even at higher approximation degrees, effectively capturing highly oscillatory solutions with high accuracy. The well-known exponential accuracy is established in the L^2 -norm, and some numerical examples are provided to demonstrate both the validity of the theoretical analysis and the efficiency of the proposed algorithm.

Keywords: Linear systems of fractional differential equations, highly oscillatory problems, Müntz-Jacobi functions, Galerkin method.

AMS subject classification: 34K37, 42B20, 65L60, 33C45.

1 Introduction

Fractional calculus (FC) has increasingly become an essential framework for modeling diverse phenomena in science and engineering. In particular, fractional differential equations (FDEs) have proven invaluable for describing processes that exhibit memory-dependent behavior. Unlike the integer-order differential equations, FDEs offer a great opportunity for modeling and simulating multi-physics phenomena. During the last few decades there has been an upsurge of intense research exploring various aspects of the theory and applications of FC and FDEs.

Kilbas et al. [26] present a detailed introduction to the theory and applications of FDEs. Diethelm [12] offers a clear introduction to FC before focusing on Caputo-type FDEs. This book contains mathematically sound theory and relevant applications. Influential works in applications include Oustaloup [31] in control theory, Hilfer [23] and Hermann [22] in physics. Podlubny [34] has become a standard reference, covering applications in mechanics, physics, and engineering. Magin [28] explores bioengineering applications, while Atanackovic et al. [2] present applications in mechanics. Baleanu et al. [3] present fractional models and numerical methods for solving FDEs. Tarasov [38] discusses applications in statistical physics, condensed matter, and quantum dynamics. Other relevant contributions can be found in the books by Ortigueira [30], Baleanu et al. [3], Petráš [33], and Sabatier et al. [35]. Mainardi [29] is a standard reference for the application of FC in viscoelasticity and wave motion, and Uchaikin [39] provides detailed motivation for FDEs in various branches of physics. Yang et al. [41],

and Gholami Bahador et al. [20, 21] successfully use fractional-order methods in image processing and image denoising.

There are diverse physical phenomena whose individual components interact closely. Consequently, the mathematical modeling of such phenomena may lead to systems of fractional differential equations (SFDEs). Due to the non-local nature of fractional derivatives, the computations involved in solving SFDEs are tedious and time consuming. Developing numerical methods for solving SFDEs has been a subject of intense research at present. Table 1 provides references for the different methods for solving SFDEs.

Type	Method	Linear	Non-linear
Single-order SFDEs	fractional Laguerre pseudo-spectral [4]	✓	✓
	Petrov-Galerkin [15]	✓	
	fractional-order Jacobi Tau [5]	✓	✓
	hybrid non-polynomial collocation [17]	✓	
	spline collocation [32]	✓	
	Jacobi-Gauss collocation [42]	✓	✓
	central part interpolation [27]	✓	
	fractional Hamiltonian boundary value [6–8]	✓	✓
Multi-order SFDEs*	Legendre wavelet [11]	✓	✓
	Bernoulli wavelet [40]	✓	✓
	Chebyshev collocation [24, 25]	✓	✓
	fractional Jacobi collocation [14]	✓	
	first kind Chebyshev Tau [1]	✓	✓
	second kind Chebyshev Tau [13]	✓	
	fractional Galerkin [16]		✓

Table 1: Summary of numerical procedures for solving SFDEs

Many existing approaches face notable drawbacks, listed below, that limit their efficiency and reliability:

- **Mismatch between basis functions and solution behavior:** The singular nature of fractional derivative operators is often not adequately addressed when selecting basis functions. As a result, many methods rely on infinitely smooth functions (such as classical polynomials) that fail to capture the solution’s actual asymptotic and regularity characteristics. Achieving truly high-order accuracy requires aligning the smoothness of the basis with the inherent behavior of the exact solution, a condition often disregarded in current literature [1, 11, 24, 25, 32, 40].
- **High computational complexity:** In much of the literature on nonlinear SFDEs and on linear SFDEs with non-constant coefficients, collocation techniques are widely used: the residual is enforced to vanish at a set of collocation points [14, 42]. This strategy typically leads to a complex nonlinear algebraic system, in the linear case, to a dense linear system. Both scenarios can impose large computational costs and may degrade the accuracy of the numerical solution. These drawbacks become more pronounced tackling highly oscillatory problems, such as certain fractional-order mechanics models, real-world problems, or problems on long domains, where satisfactory accuracy is typically achieved only at very high approximation degrees.

The goal of this research is to address these challenges by implementing a Müntz-Jacobi Galerkin

*Multi-order SFDEs refer to systems of fractional differential equations where each equation involves a fractional derivative of a distinct order.

method for solving the following class of linear SFDEs with non-constant coefficients

$$\begin{cases} D_C^{\theta_j} v_j(t) = \sum_{r=1}^n p_{j,r}(t) v_r(t) + p_{j,n+1}(t), & j = 1, 2, \dots, n, \\ v_j^{(k)}(0) = v_{j,0}^{(k)}, & k = 0, 1, \dots, \lceil \theta_j \rceil - 1, \quad t \in \Lambda = [0, T], \end{cases} \quad (1)$$

where $\theta_j = \frac{\gamma_j}{q_j} \in \mathbb{Q}^+$ with co-prime integers $\gamma_j \geq 1$ and $q_j \geq 2$, $T \in \mathbb{R}^+$ (finite), and $\lceil \cdot \rceil$ stands for the ceiling function[†]. The $p_{j,r}(t)$ are continuous functions on Λ , and $v_j(t)$ are the unknowns. $D_C^{\theta_j}$ is the Caputo fractional derivative of order θ_j , defined by

$$D_C^{\theta_j}(\cdot) = I^{\lceil \theta_j \rceil - \theta_j} \partial_x^{\lceil \theta_j \rceil}(\cdot),$$

in which $I^{\lceil \theta_j \rceil - \theta_j}$ denotes the Riemann-Liouville fractional integral operator of order $\lceil \theta_j \rceil - \theta_j$ [12,26,34].

This study presents an in-depth analysis of the regularity properties of equation (1), focusing particularly on cases where the problem exhibits highly oscillatory behavior. To tackle (1), an efficient spectral method based on Müntz-Jacobi functions, which were introduced by Shen and Wang [37], is employed, as they reflect the asymptotic behavior of the solutions of (1). Spectral techniques are well known for providing highly accurate approximations when applied to smooth problems. Nevertheless, they have certain limitations, such as the challenge of solving potentially ill-conditioned or ambiguous algebraic systems, and the significant loss of accuracy when dealing with problems that have non-smooth solutions. The approach adopted here overcomes these challenges by maintaining spectral accuracy for non-smooth and oscillatory solutions and allowing the approximate solution to be computed efficiently via recurrence relations, all without the necessity of solving complex algebraic systems.

The remainder of the paper is arranged as follows. Section 2 focuses on the regularity analysis of the solution to (1). In Section 3, we introduce the Müntz-Jacobi method for solving (1) under the assumptions of the regularity theorem. The unique solvability and computational complexity of the numerical solution are also addressed. In particular, Section 4 presents a detailed investigation of the error estimates. Finally, the numerical experiments in Section 5 demonstrate the effectiveness of our proposed algorithm and include a performance comparison with methods from the literature.

2 Regularity analysis

For the existence and uniqueness of the solution to (1), the continuity of the functions $p_{j,r}(t)$ is sufficient, and the solution inherits this continuity. This follows directly from Theorem 8.11 in [12]. The following theorem provides a series representation of the solution of (1) around the origin and specifies the conditions under which the solution exhibits highly oscillatory behavior.

Theorem 2.1 (Regularity). *Let $p_{j,r} : \mathbb{R} \rightarrow \mathbb{C}$ be periodic, highly oscillatory continuous functions of the form*

$$p_{j,r}(t) = f_{j,r}(t) e^{i\omega t}, \quad \omega \gg 1, \quad r = 1, 2, \dots, n+1,$$

which can be written as

$$p_{j,r}(t) = \bar{p}_{j,r}\left(t^{1/q}\right),$$

where $\bar{p}_{j,r}$ are analytic in a neighborhood of the origin. Then the series representation of the solution $v_j(t)$ of the equation (1), in a neighborhood of the origin, is given by

$$v_j(t) = \psi_j(t) + \sum_{\mu=\theta_j q}^{\infty} \bar{v}_{j,\mu} t^{\frac{\mu}{q}}, \quad j = 1, 2, \dots, n, \quad (2)$$

[†] $\lceil \theta_j \rceil$ denotes the smallest integer greater than or equal to θ_j .

in which $\psi_j(t) = \sum_{k=0}^{\lceil \theta_j \rceil - 1} \frac{v_{j,0}^{(k)}}{k!} t^k$, q denotes the least common multiple of the denominators q_j , and the $\bar{v}_{j,\mu}$ are known coefficients.

Proof. First we consider the following representation of $v_j(t)$

$$v_j(t) = \sum_{\mu=0}^{\infty} \bar{v}_{j,\mu} t^{\frac{\mu}{q}}, \quad j = 1, 2, \dots, n. \quad (3)$$

The unknown coefficients $\{\bar{v}_{j,\mu}\}_{j=1}^n$ are chosen such that the representation (2) converges and satisfies (1). This is accomplished by employing the series expansion of $\bar{p}_{j,r}(t^{1/q})$, $j = 1, 2, \dots, n$ around the origin, viz.

$$p_{j,r}(t) = \bar{p}_{j,r}(t^{1/q}) = \sum_{\mu_1, \mu_2=0}^{\infty} f_{j,r,\mu_1} \frac{(i\omega)^{\mu_2}}{\mu_2!} t^{\frac{\mu_1 + \mu_2}{q}}, \quad r = 1, 2, \dots, n+1. \quad (4)$$

Considering uniform convergence and substituting (3) and (4) into (1), the coefficients $\{\bar{v}_{j,\mu}\}_{j=1}^n$ satisfy the following equality

$$\begin{aligned} \sum_{\mu=0}^{\infty} \bar{v}_{j,\mu} t^{\frac{\mu}{q}} = \psi_j(t) &+ \sum_{r=1}^n \sum_{\mu_1, \mu_2=0}^{\infty} \sum_{\mu=0}^{\infty} f_{j,r,\mu_1} \bar{v}_{r,\mu} \frac{(i\omega)^{\mu_2}}{\mu_2!} I^{\theta_j} \left(t^{\frac{\mu_1 + \mu_2 + \mu}{q}} \right) \\ &+ \sum_{\mu_1, \mu=0}^{\infty} f_{j,n+1,\mu_1} \frac{(i\omega)^{\mu}}{\mu!} I^{\theta_j} \left(t^{\frac{\mu_1 + \mu}{q}} \right), \end{aligned}$$

which can be rewritten as

$$\begin{aligned} \sum_{\mu=0}^{\infty} \bar{v}_{j,\mu} t^{\frac{\mu}{q}} = \psi_j(t) &+ \sum_{r=1}^n \sum_{\mu_1, \mu_2=0}^{\infty} \sum_{\mu=0}^{\infty} f_{j,r,\mu_1} \bar{v}_{r,\mu} \xi_{1,j} \frac{(i\omega)^{\mu_2}}{\mu_2!} t^{\frac{\mu_1 + \mu_2 + \mu}{q} + \theta_j} \\ &+ \sum_{\mu_1, \mu=0}^{\infty} f_{j,n+1,\mu_1} \xi_{2,j} \frac{(i\omega)^{\mu}}{\mu!} t^{\frac{\mu_1 + \mu}{q} + \theta_j}, \end{aligned} \quad (5)$$

in which

$$\xi_{1,j} = \frac{\Gamma(\frac{\mu_1 + \mu_2 + \mu}{q} + 1)}{\Gamma(\frac{\mu_1 + \mu_2 + \mu}{q} + \theta_j + 1)}, \quad \xi_{2,j} = \frac{\Gamma(\frac{\mu_1 + \mu}{q} + 1)}{\Gamma(\frac{\mu_1 + \mu}{q} + \theta_j + 1)}.$$

Substituting $\mu = \mu - \mu_1 - \mu_2 - \theta_j q$ in the first series, and $\mu = \mu - \mu_1 - \theta_j q$ in the second series on the right-hand side of (5), we obtain

$$\begin{aligned} \sum_{\mu=0}^{\infty} \bar{v}_{j,\mu} t^{\frac{\mu}{q}} = \psi_j(t) &+ \sum_{r=1}^n \sum_{\mu_1, \mu_2=0}^{\infty} \sum_{\mu=\mu_1 + \mu_2 + \theta_j q}^{\infty} f_{j,r,\mu_1} \bar{v}_{r,\mu - \mu_1 - \mu_2 - \theta_j q} \bar{\xi}_{1,j} \frac{(i\omega)^{\mu_2}}{\mu_2!} t^{\frac{\mu}{q}} \\ &+ \sum_{\substack{\mu_1=0 \\ \mu=\mu_1 + \theta_j q}}^{\infty} f_{j,n+1,\mu_1} \bar{\xi}_{2,j} \frac{(i\omega)^{\mu - \mu_1 - \theta_j q}}{(\mu - \mu_1 - \theta_j q)!} t^{\frac{\mu}{q}}, \end{aligned} \quad (6)$$

where

$$\bar{\xi}_{1,j} = \frac{\Gamma(\frac{\mu}{q} - \theta_j + 1)}{\Gamma(\frac{\mu}{q} + 1)}, \quad \bar{\xi}_{2,j} = \frac{\Gamma(\frac{\mu}{q} - \theta_j + 1)}{\Gamma(\frac{\mu}{q} + 1)}.$$

In this step, we compare the coefficients of $t^{\frac{\mu}{q}}$ on both sides of (6) to determine the unknown coefficients $\bar{v}_{j,\mu}$. For $\mu < \theta_j q$, it is straightforward to observe that

$$\bar{v}_{j,\mu} = \begin{cases} \frac{v_{j,0}^{(\frac{\mu}{q})}}{(\frac{\mu}{q})!}, & \mu = 0, q, \dots, (\lceil \theta_j \rceil - 1)q, \\ 0, & \text{else,} \end{cases}$$

and for $\mu \geq \theta_j q$, we find

$$\bar{v}_{j,\mu} = \sum_{r=1}^n \sum_{\mu_1, \mu_2=0}^{\infty} f_{j,r,\mu_1} \bar{v}_{r,\mu-\mu_1-\mu_2-\theta_j q} \bar{\xi}_{1,j} \frac{(i\omega)^{\mu_2}}{\mu_2!} + \sum_{\mu_1=0}^{\infty} f_{j,n+1,\mu_1} \bar{\xi}_{2,j} \frac{(i\omega)^{\mu-\mu_1-\theta_j q}}{(\mu-\mu_1-\theta_j q)!}. \quad (7)$$

We see that this is a recurrence relation: It states that its left-hand side, viz. $\bar{v}_{j,\mu}$, only depends on coefficients $\bar{v}_{j,\mu-\mu_1-\mu_2-\theta_j q}$ where

$$0 \leq \mu - \mu_1 - \mu_2 - \theta_j q < \mu.$$

This shows that the series representation (2) provides a unique solution to the main problem (1). Moreover, its uniform and absolute convergence in a neighborhood of the origin is a consequence of Theorem 3.2 in [14]. \square

Theorem 2.1 leads to the following series expansion of $v_j(t)$.

Corollary 2.2. *Under the assumptions of Theorem 2.1, we have*

$$v_j(t) = \psi_j(t) + \sum_{\mu=\theta_j q}^{\infty} \mathbf{G}_{\mu-\theta_j q}(i\omega) t^{\frac{\mu}{q}}, \quad j = 1, 2, \dots, n, \quad (8)$$

where $\mathbf{G}_{\mu-\theta_j q}(i\omega) = \sum_{k=0}^{\mu-\theta_j q} a_{j,k} \frac{(i\omega)^k}{k!}$, and the coefficients $a_{j,k}$ depend on the data $\{f_{j,r,\mu_1}\}$, the parameters $\{\bar{\xi}_{\ell,j}\}_{\ell=1}^2$, and the known coefficients $\{\bar{v}_{r,\nu}\}$, $\nu < \mu$.

Proof. This follows directly from Theorem 2.1 upon substituting (7) into (2). \square

To clarify the structure of the series expansions (2) and (8), we give the following example.

Example 2.1. *Consider the system (1) with fractional orders $\theta_1 = \frac{1}{2}$ and $\theta_2 = \frac{3}{2}$, together with the initial data $v_{1,0}^{(0)}$, $v_{2,0}^{(0)}$, and $v_{2,0}^{(1)}$. The given force functions are assumed to be continuous and highly oscillatory of the form*

$$p_{j,r}(t) = f_{j,r}(t) e^{i\omega t}, \quad \omega \gg 1, \quad j = 1, 2, \quad r = 1, 2, 3.$$

In this setting $q = 2$ and the solutions $v_1(t)$ and $v_2(t)$ admit the following series representations

$$v_1(t) = \psi_1(t) + \sum_{\mu=1}^{\infty} \bar{v}_{1,\mu} t^{\frac{\mu}{2}}, \quad v_2(t) = \psi_2(t) + \sum_{\mu=3}^{\infty} \bar{v}_{2,\mu} t^{\frac{\mu}{2}}, \quad (9)$$

where $\psi_1(t) = v_{1,0}^{(0)}$ and $\psi_2(t) = v_{2,0}^{(0)} + v_{2,0}^{(1)}t$. Following (7), the coefficients $\bar{v}_{1,\mu}$ for $\mu \geq 1$, and $\bar{v}_{2,\mu}$ for $\mu \geq 3$, satisfy recursive relations of the form

$$\begin{aligned} \bar{v}_{1,\mu} &= \sum_{r=1}^2 \sum_{\mu_1, \mu_2=0}^{\infty} f_{1,r,\mu_1} \bar{v}_{r,\mu-\mu_1-\mu_2-1} \bar{\xi}_{1,1} \frac{(i\omega)^{\mu_2}}{\mu_2!} + \sum_{\mu_1=0}^{\infty} f_{1,3,\mu_1} \bar{\xi}_{2,1} \frac{(i\omega)^{\mu-\mu_1-1}}{(\mu-\mu_1-1)!}, \\ \bar{v}_{2,\mu} &= \sum_{r=1}^2 \sum_{\mu_1, \mu_2=0}^{\infty} f_{2,r,\mu_1} \bar{v}_{r,\mu-\mu_1-\mu_2-3} \bar{\xi}_{1,2} \frac{(i\omega)^{\mu_2}}{\mu_2!} + \sum_{\mu_1=0}^{\infty} f_{2,3,\mu_1} \bar{\xi}_{2,2} \frac{(i\omega)^{\mu-\mu_1-3}}{(\mu-\mu_1-3)!}. \end{aligned}$$

Substituting $\bar{v}_{1,\mu}$ and $\bar{v}_{2,\mu}$ into (9) yields the representation (8).

$$\begin{aligned} v_1(t) &= \psi_1(t) + \mathbf{G}_{1,0}(i\omega) t^{\frac{1}{2}} + \mathbf{G}_{1,1}(i\omega) t + \mathbf{G}_{1,2}(i\omega) t^{\frac{3}{2}} + \dots, \\ v_2(t) &= \psi_2(t) + \mathbf{G}_{2,0}(i\omega) t^{\frac{3}{2}} + \mathbf{G}_{2,1}(i\omega) t^2 + \mathbf{G}_{2,2}(i\omega) t^{\frac{5}{2}} + \dots, \end{aligned}$$

where

$$\mathbf{G}_{1,\mu-1}(i\omega) = \sum_{k=0}^{\mu-1} a_{1,k} \frac{(i\omega)^k}{k!}, \quad \mathbf{G}_{2,\mu-3}(i\omega) = \sum_{k=0}^{\mu-3} a_{2,k} \frac{(i\omega)^k}{k!}.$$

From Corollary 2.2 it follows that the solutions of (1) not only inherit the reduced regularity of the functions $p_{j,r}(t)$ at the origin (the derivative of order $\lceil \theta_j \rceil$ of $v_j(t)$ may be discontinuous there), but also their highly oscillatory behavior. This combination of reduced regularity and oscillations makes the design of high-order spectral methods particularly challenging. Achieving an accurate approximation requires a careful choice of basis functions that reproduce the asymptotic behavior of the exact solutions, since standard infinitely smooth bases fail in this setting. In addition, stability considerations are crucial, because the method can attain high accuracy only for sufficiently large approximation degrees, where the oscillatory nature of the solution becomes dominant. In the following section, we construct our numerical approach under the assumptions of Theorem 2.1 in order to address these difficulties.

3 Numerical method

This section presents the Müntz-Jacobi Galerkin method. We begin with an introduction to Müntz-Jacobi functions [37], which play a key role in the subsequent development.

3.1 Müntz-Jacobi functions

First, we recall the shifted Jacobi polynomials $J_i^{(\alpha,\beta)}(s)$ for $\alpha, \beta > -1$, which form an orthogonal system on $I = [0, 1]$ with respect to the weight function $w^{(\alpha,\beta)}(s) = s^\beta(1-s)^\alpha$ [36]

$$(J_i^{(\alpha,\beta)}, J_j^{(\alpha,\beta)})_{w^{(\alpha,\beta)}} = \int_I J_i^{(\alpha,\beta)}(s) J_j^{(\alpha,\beta)}(s) w^{(\alpha,\beta)}(s) ds = \zeta_i^{(\alpha,\beta)} \delta_{ij}, \quad i, j \geq 0,$$

where

$$\zeta_i^{(\alpha,\beta)} = \|J_i^{(\alpha,\beta)}\|_{w^{(\alpha,\beta)}}^2 = \frac{\Gamma(i+\alpha+1)\Gamma(i+\beta+1)}{(2i+\alpha+\beta+1)i!\Gamma(i+\alpha+\beta+1)}.$$

Here, δ_{ij} denotes the Kronecker delta, while $(\cdot, \cdot)_{w^{(\alpha,\beta)}}$ and $\|\cdot\|_{w^{(\alpha,\beta)}}$ represent the weighted L^2 inner product and norm, respectively. For simplicity, we write (\cdot, \cdot) and $\|\cdot\|$ when $\alpha = \beta = 0$. These polynomials also admit the following explicit representation

$$J_i^{(\alpha,\beta)}(s) = \sum_{j=0}^i \Upsilon_j^{(\alpha,\beta,i)} s^j,$$

where

$$\Upsilon_j^{(\alpha,\beta,i)} = \frac{(-1)^{i-j} \Gamma(i+\beta+1) \Gamma(i+\alpha+\beta+j+1)}{\Gamma(\beta+j+1) j! \Gamma(i+\alpha+\beta+1) (i-j)!}.$$

- Considering $\Lambda = \{\lambda_\ell = \ell\eta\}_{\ell=0}^\infty$, $\eta \in (0, 1)$, we define the Müntz space associated with Λ as

$$\mathbf{M}_N(\Lambda) = \text{span}\{t^{\lambda_0}, t^{\lambda_1}, \dots, t^{\lambda_N}\}, \quad \mathbf{M}(\Lambda) = \bigcup_{N=0}^\infty \mathbf{M}_N(\Lambda).$$

We introduce the one-to-one mapping $I \rightarrow I$ by

$$u = u(s) = s^{\frac{1}{\eta}}, \quad s = s(u) = u^\eta.$$

The Müntz-Jacobi function with index $(0, \frac{1}{\eta} - 1)$ is defined by

$$\mathcal{J}_i^{(0, \frac{1}{\eta} - 1)}(u) = J_i^{(0, \frac{1}{\eta} - 1)}(s(u)), \quad i = 0, 1, \dots, \quad (10)$$

where $J_i^{(0, \frac{1}{\eta}-1)}(\cdot)$ is the shifted Jacobi polynomial with index $(0, \frac{1}{\eta} - 1)$. Using the explicit formula of shifted Jacobi polynomials, we obtain

$$\mathcal{J}_i^{(0, \frac{1}{\eta}-1)}(u) = \sum_{j=0}^i \Upsilon_j^{(0, \frac{1}{\eta}-1, i)} u^{j\eta} \in \mathbf{M}_i(\Lambda),$$

where

$$\Upsilon_j^{(0, \frac{1}{\eta}-1, i)} = \frac{(-1)^{i-j} \Gamma(i + \frac{1}{\eta}) \Gamma(i + \frac{1}{\eta} + j)}{\Gamma(\frac{1}{\eta} + j) j! \Gamma(i + \frac{1}{\eta})(i - j)!}.$$

- The Müntz-Jacobi functions $\{\mathcal{J}_i^{(0, \frac{1}{\eta}-1)}(u)\}$ are mutually $L^2(I)$ -orthogonal, i.e.,

$$\int_I \mathcal{J}_i^{(0, \frac{1}{\eta}-1)}(u) \mathcal{J}_j^{(0, \frac{1}{\eta}-1)}(u) du = \hat{\zeta}_i^{(0, \frac{1}{\eta}-1)} \delta_{ij}, \quad i, j \geq 0,$$

where $\hat{\zeta}_i^{(0, \frac{1}{\eta}-1)} = \frac{1}{\eta} \zeta_i^{(0, \frac{1}{\eta}-1)}$. These functions form a complete orthogonal system in $L^2(I)$. That is, for each $v(u) \in L^2(I)$, we have the following unique expansion

$$v(u) = \sum_{i=0}^{\infty} c_i \mathcal{J}_i^{(0, \frac{1}{\eta}-1)}(u), \quad c_i = \frac{(v, \mathcal{J}_i^{(0, \frac{1}{\eta}-1)})}{\|\mathcal{J}_i^{(0, \frac{1}{\eta}-1)}\|^2}.$$

Therefore, we have

$$\mathbf{M}_N(\Lambda) = \text{span}\{\mathcal{J}_0^{(0, \frac{1}{\eta}-1)}(u), \mathcal{J}_1^{(0, \frac{1}{\eta}-1)}(u), \dots, \mathcal{J}_N^{(0, \frac{1}{\eta}-1)}(u)\}.$$

- The Müntz-Jacobi orthogonal projection $\pi_N : L^2(I) \rightarrow \mathbf{M}_N(\Lambda)$ is stated by

$$\pi_N v = \sum_{i=0}^N c_i \mathcal{J}_i^{(0, \frac{1}{\eta}-1)}(u),$$

which has the following property

$$(v - \pi_N v, \phi) = 0, \quad \forall \phi \in \mathbf{M}_N(\Lambda).$$

We now derive an estimate for the truncation error $\pi_N v - v$. For this purpose, assume that the functions $v(u)$ and $V(s)$ are related by $v(u) = V(s(u))$. Thus, their derivatives are connected as follows

$$\begin{aligned} D_u v &:= \partial_s V(s) = \partial_s u \partial_u v, \\ D_u^2 v &:= \partial_s^2 V(s) = \partial_s u \partial_u (D_u v), \\ &\vdots \\ D_u^k v &:= \partial_s^k V(s) = \partial_s u \partial_u (\partial_s u \partial_u (\dots (\partial_s u \partial_u v) \dots)), \end{aligned} \tag{11}$$

in which $\partial_s u = \frac{1}{\eta}(u)^{1-\eta}$.

Now, we define the space

$$H_{\hat{w}^{(0,0)}}^k(I) = \{v : \|v\|_{k, \hat{w}^{(0,0)}} < \infty\},$$

with the associated norm and semi-norm

$$\|v\|_{k, \hat{w}^{(0,0)}}^2 = \sum_{\ell=0}^k \|D_u^\ell v\|_{\hat{w}^{(\ell, \ell)}}^2, \quad |v|_{k, \hat{w}^{(0,0)}} = \|D_u^k v\|_{\hat{w}^{(k, k)}},$$

in which $\hat{w}^{(\alpha, \beta)}(u) = w^{(\alpha, \beta)}(s(u))^\ddagger$.

Next, we state a theorem that provides an upper bound for the truncation error $\pi_N v - v$.

[‡]Note that $\hat{w}^{(0,0)}(u) = w^{(0,0)}(s(u)) = 1$, and therefore $\|\cdot\|_{\hat{w}^{(0,0)}}$ is simply the L^2 -norm with the constant weight 1.

Theorem 3.1. [37, Theorem 3.3] It follows that, for some $C > 0$ independent of N ,

$$\|\pi_N v - v\|_{\hat{w}(0,0)} \leq CN^{-k} |v|_{k, \hat{w}(0,0)},$$

where $v \in H_{\hat{w}(0,0)}^k(I)$ and $k \in \mathbb{N}$.

Further properties of the Müntz-Jacobi functions can be found in the work of Shen and Wang [37].

3.2 Müntz-Jacobi Galerkin algorithm

We proceed to implement the numerical scheme and examine its computational complexity.

By applying I^{θ_j} to both sides of (1) and using $I^{\theta_j} D_C^{\theta_j} v_j(t) = v_j(t) - \psi_j(t)$, the equation (1) can be rewritten as the following system of Volterra integral equations

$$v_j(t) = \psi_j(t) + \sum_{r=1}^n I^{\theta_j} (p_{j,r}(t) v_r(t)) + I^{\theta_j} (p_{j,n+1}(t)), \quad j = 1, 2, \dots, n. \quad (12)$$

Under the coordinate transformation $t = Tu$, the equation (12) is transformed into the following system of equations on I

$$\bar{v}_j(u) = \bar{\psi}_j(u) + T^{\theta_j} \sum_{r=1}^n I^{\theta_j} (\bar{p}_{j,r}(u) \bar{v}_r(u)) + T^{\theta_j} I^{\theta_j} (\bar{p}_{j,n+1}(u)), \quad j = 1, 2, \dots, n, \quad (13)$$

where $\bar{v}_j(u) = v_j(Tu)$, $\bar{\psi}_j(u) = \psi_j(Tu)$, and $\bar{p}_{j,r}(u) = p_{j,r}(Tu)$, $j = 1, 2, \dots, n$, $r = 1, 2, \dots, n+1$. By setting $\eta = \frac{1}{q}$ in (10), the Müntz-Jacobi functions $\{\mathcal{J}_i^{(0,q-1)}\}_{i \geq 0}$ are obtained as follows

$$\mathcal{J}_i^{(0,q-1)}(u) = J_i^{(0,q-1)}(s(u)) = \text{span}\{1, u^\eta, \dots, u^{i\eta}\}. \quad (14)$$

Now, we present a highly accurate Galerkin solution $\bar{v}_{j,N}(u)$ to the transformed equation (13) where the Müntz-Jacobi functions $\{\mathcal{J}_i^{(0,q-1)}\}_{i \geq 0}$ introduced in (14) are employed as basis functions. In this regard, we consider the Galerkin solution of (13) as

$$\bar{v}_{j,N}(u) = \sum_{i=0}^{\infty} c_{j,i} \mathcal{J}_i^{(0,q-1)}(u) = \underline{c}_j \underline{\mathcal{J}}^{(0,q-1)} = \underline{c}_j \mathcal{J} \underline{U}_u, \quad j = 1, 2, \dots, n, \quad (15)$$

where $\underline{\mathcal{J}}^{(0,q-1)} = [\mathcal{J}_0^{(0,q-1)}(u), \mathcal{J}_1^{(0,q-1)}(u), \dots, \mathcal{J}_N^{(0,q-1)}(u), \dots]^T$ is the vector of Müntz-Jacobi functions with degree $(\mathcal{J}_i^{(0,q-1)}(u)) \leq i\eta$, and $\underline{c}_j = [c_{j,0}, c_{j,1}, \dots, c_{j,N}, 0, \dots]$. Also, \mathcal{J} is an invertible lower triangular matrix, and $\underline{U}_u = [1, u^\eta, \dots, u^{N\eta}, \dots]^T$. In addition, we suppose that

$$\begin{aligned} \bar{\psi}_j(u) &= \sum_{i=0}^{\infty} \bar{\psi}_{j,i} u^{i\eta} = \underline{\bar{\psi}}_j \underline{U}_u, \quad \underline{\bar{\psi}}_j = [\bar{\psi}_{j,0}, \bar{\psi}_{j,1}, \dots, \bar{\psi}_{j,N}, 0, \dots], \\ \bar{p}_{j,r}(u) &= \bar{p}_{j,r,N}(u) = \sum_{i=0}^{\infty} p_{j,r,i} \mathcal{J}_i^{(0,q-1)}(u) \\ &= \underline{p}_{j,r} \mathcal{J} \underline{U}_u = \hat{\underline{p}}_{j,r} \underline{U}_u = \sum_{i=0}^{\infty} \hat{p}_{j,r,i} u^{i\eta}, \quad j = 1, 2, \dots, n, \quad r = 1, 2, \dots, n+1, \end{aligned} \quad (16)$$

in which $\underline{p}_{j,r} = [p_{j,r,0}, p_{j,r,1}, \dots, p_{j,r,N}, 0, \dots]$, and $\hat{\underline{p}}_{j,r} = [\hat{p}_{j,r,0}, \hat{p}_{j,r,1}, \dots, \hat{p}_{j,r,N}, 0, \dots]$. Substituting (15) and (16) into (13) yields

$$\begin{aligned} \underline{c}_j \mathcal{J} \underline{U}_u &= \underline{\bar{\psi}}_j \underline{U}_u + T^{\theta_j} \sum_{r=1}^n \underline{c}_r \mathcal{J} \left(\sum_{i=0}^{\infty} \hat{p}_{j,r,i} I^{\theta_j} (u^{i\eta} \underline{U}_u) \right) \\ &+ T^{\theta_j} \hat{\underline{p}}_{j,n+1} I^{\theta_j} (\underline{U}_u), \quad j = 1, 2, \dots, n. \end{aligned} \quad (17)$$

Therefore, it suffices to compute $I^{\theta_j} (u^{i\eta} \underline{U}_u)$, and $I^{\theta_j} (\underline{U}_u)$. Consequently, by $I^\alpha u^\beta = \text{frac}\Gamma(\beta + 1)\Gamma(\alpha + \beta + 1)u^{\alpha+\beta}$, we arrive at

$$\begin{aligned} I^{\theta_j} (u^{i\eta} \underline{U}_u) &= \left\{ I^{\theta_j} \left(u^{(i+m)\eta} \right) \right\}_{m=0}^{\infty} = \left\{ \xi_{j,i}^m u^{(i+m)\eta+\theta_j} \right\}_{m=0}^{\infty}, \\ I^{\theta_j} (\underline{U}_u) &= \left\{ I^{\theta_j} (u^{m\eta}) \right\}_{m=0}^{\infty} = \left\{ \vartheta_j^m u^{m\eta+\theta_j} \right\}_{m=0}^{\infty} = Q_j \underline{U}_u, \end{aligned} \quad (18)$$

where $\xi_{j,i}^m = \frac{\Gamma((i+m)\eta+1)}{\Gamma((i+m)\eta+\theta_j+1)}$, $\vartheta_j^m = \frac{\Gamma(m\eta+1)}{\Gamma(m\eta+\theta_j+1)}$ and

$$Q_j = \begin{bmatrix} \overbrace{0 \dots 0}^{\theta_j q} & \vartheta_j^0 & 0 & \dots & & \\ \vdots & 0 & \vartheta_j^1 & 0 & \dots & \\ \vdots & \vdots & 0 & \vartheta_j^2 & 0 & \dots \\ \dots & \dots & & \ddots & \ddots & \ddots \end{bmatrix}.$$

For $j = 1, 2, \dots, n$, inserting (18) into (17) concludes

$$\begin{aligned} \underline{c}_j \mathcal{J} \underline{U}_u &= \underline{\psi}_j \underline{U}_u + T^{\theta_j} \sum_{r=1}^n \underline{c}_r \mathcal{J} \left(\sum_{i=0}^{\infty} \hat{p}_{j,r,i} \left\{ \xi_{j,i}^m u^{(i+m)\eta+\theta_j} \right\}_{m=0}^{\infty} \right) \\ &+ T^{\theta_j} \hat{p}_{j,n+1} Q_j \underline{U}_u. \end{aligned} \quad (19)$$

The relation (19) can be rewritten as

$$\underline{c}_j \mathcal{J} \underline{U}_u = \underline{\psi}_j \underline{U}_u + \sum_{r=1}^n \underline{c}_r \mathcal{J} A_{j,r} \underline{U}_u + T^{\theta_j} \hat{p}_{j,n+1} Q_j \underline{U}_u, \quad (20)$$

in which $A_{j,r}$, $j, r = 1, 2, \dots, n$ are infinite upper-triangular matrices with the following entries

$$(A_{j,r})_{k,\ell=0}^{\infty} = \begin{cases} 0, & k \geq \ell - \theta_j q + 1, \\ T^{\theta_j} \hat{p}_{j,r,\ell-k-\theta_j q} \xi_{j,\ell-k-\theta_j q}^k, & k < \ell - \theta_j q + 1. \end{cases} \quad (21)$$

Projecting (20) onto $\{\mathcal{J}_i^{(0,q-1)}\}_{i=0}^N$ and using the orthogonality property of the Müntz-Jacobi functions implies

$$\underline{c}_j^N = \left(\underline{\psi}_j^N + \sum_{r=1}^n \underline{c}_r^N \mathcal{J}^N A_{j,r}^N + T^{\theta_j} \hat{p}_{j,n+1}^N Q_j^N \right) (\mathcal{J}^N)^{-1}. \quad (22)$$

The matrices and vectors with the index N on top correspond to the sub-matrices and sub-vectors of order $N + 1$, respectively. The unknown vectors are then obtained by solving the corresponding $n(N + 1) \times n(N + 1)$ system of algebraic equations (22).

3.3 Numerical solvability and complexity analysis

The main object of this section is to provide a theorem which reveals that the algebraic system (22) has a unique solution and to propose a well-posed strategy to solve it.

Theorem 3.2. *The linear algebraic system (22) has a unique solution obtained by a determined recurrence relation.*

Proof. Multiplying both sides of (22) by \mathcal{J}^N , and defining

$$\tilde{\underline{c}}_j^N = \underline{c}_j^N \mathcal{J}^N = [\tilde{c}_{j,0}, \tilde{c}_{j,1}, \dots, \tilde{c}_{j,N}], \quad (23)$$

we can rewrite (22) as

$$\tilde{\underline{c}}_j^N = \sum_{r=1}^n \tilde{\underline{c}}_r^N A_{j,r}^N + \underline{P}_j, \quad j = 1, 2, \dots, n, \quad (24)$$

in which

$$\underline{P}_j = \underline{\psi}_j^N + T^{\theta_j} \hat{\underline{p}}_{j,n+1}^N Q_j^N = [P_{j,0}, P_{j,1}, \dots, P_{j,N}].$$

Next, exploiting the structure of the upper-triangular matrix $(A_{j,r})_N$ defined in (21), we have

$$\tilde{\underline{c}}_r^N (A_{j,r})^N = \tilde{\underline{c}}_r^N \begin{bmatrix} \overbrace{0 \dots 0}^{\theta_j q} & (A_{j,r})_{0,\theta_j q} & (A_{j,r})_{0,\theta_j q+1} & \dots & (A_{j,r})_{0,N} \\ \vdots & 0 & (A_{j,r})_{1,\theta_j q+1} & \dots & (A_{j,r})_{1,N} \\ \vdots & \vdots & \vdots & \ddots & \ddots \\ 0 & 0 & \ddots & 0 & (A_{j,r})_{N-\theta_j q,N} \\ \vdots & \vdots & \vdots & \ddots & \vdots \\ 0 & 0 & 0 & 0 & 0 \end{bmatrix}.$$

From the relation above, it follows that

$$\begin{aligned} (\tilde{\underline{c}}_r^N (A_{j,r})^N)_{\ell=0}^N &= \begin{cases} 0, & \ell < \theta_j q, \\ \sum_{k=0}^{\ell-\theta_j q} \tilde{c}_{r,k} (A_{j,r})_{k,\ell}, & \ell \geq \theta_j q, \end{cases} \\ &= [\overbrace{0 \dots 0}^{\theta_j q}, \mathbf{F}_{\theta_j q}^{j,r}(\tilde{c}_{r,0}), \mathbf{F}_{\theta_j q+1}^{j,r}(\tilde{c}_{r,0}, \tilde{c}_{r,1}), \dots, \mathbf{F}_N^{j,r}(\tilde{c}_{r,0}, \tilde{c}_{r,1}, \dots, \tilde{c}_{r,N-\theta_j q})], \end{aligned} \quad (25)$$

where

$$\mathbf{F}_m^{j,r}(\tilde{c}_{r,0}, \tilde{c}_{r,1}, \dots, \tilde{c}_{r,m-\theta_j q}), \quad \theta_j q \leq m \leq N,$$

are linear functions of the elements $\tilde{c}_{r,0}, \tilde{c}_{r,1}, \dots, \tilde{c}_{r,m-\theta_j q}$. Inserting (25) into (24), it can be concluded that the unknown components of the unknown vectors $\{\tilde{\underline{c}}_j^N\}_{j=1}^n$ are calculated by the following recurrence relations

$$\begin{aligned} \tilde{c}_{j,0} &= P_{j,0}, \dots, \tilde{c}_{j,\theta_j q-1} = P_{j,\theta_j q-1}, \\ \tilde{c}_{j,\theta_j q} &= \sum_{r=1}^n \mathbf{F}_{\theta_j q}^{j,r}(\tilde{c}_{r,0}) + P_{j,\theta_j q}, \\ &\vdots \\ \tilde{c}_{j,N} &= \sum_{r=1}^n \mathbf{F}_N^{j,r}(\tilde{c}_{r,0}, \tilde{c}_{r,1}, \dots, \tilde{c}_{r,N-\theta_j q}) + P_{j,N}, \end{aligned} \quad (26)$$

which implies the result. \square

In fact, the direct solution of the $n(N+1) \times n(N+1)$ system of algebraic equations (22) can yield inaccurate approximations, due to the increased computational cost and the possibility of increasing the condition number of the coefficient matrix, especially for a large degree of approximation N . Accordingly, we avoid solving the system of algebraic equations (22) directly, and compute the unknowns

by recurrence relations.

Finally, upon solving the lower triangular system (23) to determine $\{\underline{c}_j^N\}_{j=1}^n$, the corresponding Müntz-Jacobi Galerkin solutions (15) are obtained. Then the approximate solutions $v_{j,N}(t)$ of the main problem (1) are given by

$$v_{j,N}(t) = \bar{v}_{j,N}\left(\frac{t}{T}\right), \quad j = 1, 2, \dots, n.$$

4 Error analysis

This section is devoted to analyzing the convergence of the proposed method by deriving an appropriate error bound in a weighted L^2 -norm.

Theorem 4.1 (Error estimate). *Suppose that $\bar{v}_{j,N}(u)$ given by (15) are the approximate solutions of (13). If the following conditions satisfy*

1. $D_u^{\epsilon_{jr}+1}(I^{\theta_j}(\bar{p}_{j,r}(u)\bar{v}_r(u))) \in C(I)$,
2. $I^{\theta_j}(\bar{p}_{j,r}(u)\bar{v}_r(u)) \in H_{\hat{w}(0,0)}^{\epsilon_{jr}}(I)$, $\epsilon_{jr} \geq 0$,
3. $I^{\theta_j}(\bar{p}_{j,n+1}(u)) \in H_{\hat{w}(0,0)}^{\rho_j}(I)$, $\rho_j \geq 0$,

then for sufficiently large values of N we have

$$\|\bar{e}_{j,N}(u)\|_{\hat{w}(0,0)} \leq C \left(N^{-\epsilon_{jr}} |I^{\theta_j}(\bar{p}_{j,r}(u)\bar{v}_r(u))|_{\epsilon_{jr}, \hat{w}(0,0)} + N^{-\rho_j} |I^{\theta_j}(\bar{p}_{j,n+1}(u))|_{\rho_j, \hat{w}(0,0)} \right),$$

where $\bar{e}_{j,N}(u) = \bar{v}_j(u) - \bar{v}_{j,N}(u)$ denotes the error function, and $C > 0$ is a constant independent of N .

Proof. According to the proposed numerical scheme in Section 3, we have

$$\bar{v}_{j,N}(u) = \bar{\psi}_j(u) + T^{\theta_j} \sum_{r=1}^n I^{\theta_j}(\bar{p}_{j,r}(u)\bar{v}_{r,N}(u)) + T^{\theta_j} I^{\theta_j}(\bar{p}_{j,n+1}(u)), \quad j = 1, 2, \dots, n. \quad (27)$$

Then, following the same approach used to derive (22), we multiply both sides of (27) by $\mathcal{J}_i^{(0,q-1)}(u)$ and integrate over I , which yields

$$(\bar{v}_{j,N} - \bar{\psi}_j - T^{\theta_j} \sum_{r=1}^n I^{\theta_j}(\bar{p}_{j,r}\bar{v}_{r,N}) - T^{\theta_j} I^{\theta_j}(\bar{p}_{j,n+1}), \mathcal{J}_i^{(0,q-1)}) = 0, \quad i = 0, 1, \dots, N. \quad (28)$$

Now, multiplying both sides of (28) by $\{\frac{\mathcal{J}_i^{(0,q-1)}(u)}{\zeta_i^{(0,q-1)}}\}_{i=0}^N$ and summing up from $i = 0$ to $i = N$, one arrives at

$$\pi_N(\bar{v}_{j,N} - \bar{\psi}_j - T^{\theta_j} \sum_{r=1}^n I^{\theta_j}(\bar{p}_{j,r}\bar{v}_{r,N}) - T^{\theta_j} I^{\theta_j}(\bar{p}_{j,n+1})) = 0,$$

which is equivalent to

$$\bar{v}_{j,N}(u) = \bar{\psi}_j(u) + T^{\theta_j} \sum_{r=1}^n \pi_N(I^{\theta_j}(\bar{p}_{j,r}\bar{v}_{r,N})) + T^{\theta_j} \pi_N(I^{\theta_j}(\bar{p}_{j,n+1})), \quad (29)$$

since we have $\bar{v}_{j,N}(u), \bar{\psi}_j(u) \in \text{span}\{\mathcal{J}_0^{(0,q-1)}, \mathcal{J}_1^{(0,q-1)}, \dots, \mathcal{J}_N^{(0,q-1)}\}$. Subtracting (29) from (13) yields

$$\begin{aligned} \bar{e}_{j,N}(u) = T^{\theta_j} \sum_{r=1}^n I^{\theta_j}(\bar{p}_{j,r}(u)\bar{v}_r(u)) & - T^{\theta_j} \sum_{r=1}^n \pi_N(I^{\theta_j}(\bar{p}_{j,r}(u)\bar{v}_{r,N}(u))) \\ & + T^{\theta_j} I^{\theta_j}(\bar{p}_{j,n+1}(u)) - T^{\theta_j} \pi_N(I^{\theta_j}(\bar{p}_{j,n+1}(u))), \end{aligned}$$

which can be rewritten in the following sense

$$\bar{e}_{j,N}(u) = T^{\theta_j} \sum_{r=1}^n \Gamma^{r_j} (\bar{p}_{j,r}(u) \bar{e}_{r,N}(u)) + \Pi_j. \quad (30)$$

Equivalently we obtain

$$\bar{e}_{j,N}(u) = \sum_{r=1}^n \left(\int_0^u k_{j,r}(u, w) \bar{e}_{r,N}(w) dw \right) + \Pi_j,$$

where $k_{j,r}(u, w) = \frac{T^{\theta_j}}{\Gamma(\theta_j)} (u - w)^{\theta_j - 1} \bar{p}_{j,r}(u)$, and

$$\Pi_j = T^{\theta_j} \sum_{r=1}^n e_{\pi_N} \left(I^{\theta_j} (\bar{p}_{j,r}(u) \bar{v}_{r,N}(u)) \right) + T^{\theta_j} e_{\pi_N} \left(I^{\theta_j} (\bar{p}_{j,n+1}(u)) \right).$$

Here, $e_{\pi_N}(f) = f - \pi_N(f)$. Defining the vectors

$$\underline{E}(u) = [\bar{e}_{1,N}(u), \bar{e}_{2,N}(u), \dots, \bar{e}_{n,N}(u)]^T, \quad \underline{\Pi} = [\Pi_1, \Pi_2, \dots, \Pi_n]^T,$$

we can rewrite the equation (30) as the following matrix formulation

$$\underline{E}(u) = \int_0^u (u - w)^{\min_{1 \leq i \leq n} \{\theta_i\} - 1} K(u, w) \underline{E}(w) dw + \underline{\Pi}, \quad (31)$$

where

$$\begin{aligned} K(u, w) &= \left((u - w)^{1 - \min_{1 \leq i \leq n} \{\theta_i\}} k_{j,r}(u, w) \right)_{j,r=1}^n \\ &= \left(\frac{T^{\theta_j}}{\Gamma(\theta_j)} (u - w)^{\theta_j - \min_{1 \leq i \leq n} \{\theta_i\}} \bar{p}_{j,r}(u) \right)_{j,r=1}^n, \end{aligned}$$

is a continuous function on $\{(u, w) : 0 \leq w \leq u \leq 1\}$. From (31), it follows that

$$|\underline{E}| \leq \Psi \int_0^u (u - w)^{\min_{1 \leq i \leq n} \{\theta_i\} - 1} |\underline{E}(w)| dw + |\underline{\Pi}|,$$

where $\Psi = \max_{0 \leq w \leq u \leq 1} |K(u, w)| < \infty$. Applying Gronwall's inequality, i.e., Lemma 6 of [13] leads to

$$\|\underline{E}\|_{\hat{w}(0,0)} \leq C \|\underline{\Pi}\|_{\hat{w}(0,0)},$$

and consequently

$$\begin{aligned} \|\bar{e}_{j,N}(u)\|_{\hat{w}(0,0)} &\leq C \|\Pi_j\|_{\hat{w}(0,0)} \\ &\leq C \left(\sum_{r=1}^n \|e_{\pi_N} \left(I^{\theta_j} (\bar{p}_{j,r}(u) \bar{v}_{r,N}(u)) \right)\|_{\hat{w}(0,0)} \right. \\ &\quad \left. + \|e_{\pi_N} \left(I^{\theta_j} (\bar{p}_{j,n+1}(u)) \right)\|_{\hat{w}(0,0)} \right). \end{aligned} \quad (32)$$

Using Theorem 3.1, we deduce

$$\begin{aligned} \|e_{\pi_N} \left(I^{\theta_j} (\bar{p}_{j,r}(u) \bar{v}_{r,N}(u)) \right)\|_{\hat{w}(0,0)} &\leq CN^{-\epsilon_{jr}} |I^{\theta_j} (\bar{p}_{j,r}(u) \bar{v}_{r,N}(u))|_{\epsilon_j, \hat{w}(0,0)} \\ &\leq CN^{-\epsilon_{jr}} \left(|I^{\theta_j} (\bar{p}_{j,r}(u) \bar{v}_r(u))|_{\epsilon_{jr}, \hat{w}(0,0)} \right. \\ &\quad \left. + \|D_u (D_u^{\epsilon_{jr}} I^{\theta_j} (\bar{p}_{j,r}(u) \bar{v}_r(u)))\|_{\infty} \|\bar{e}_{r,N}\|_{\hat{w}(0,0)} \right) \\ &\leq CN^{-\epsilon_{jr}} \left(|I^{\theta_j} (\bar{p}_{j,r}(u) \bar{v}_r(u))|_{\epsilon_{jr}, \hat{w}(0,0)} + \|\bar{e}_{r,N}\|_{\hat{w}(0,0)} \right), \end{aligned} \quad (33)$$

where follows from the use of the first assumption together with the first order Taylor formula. Again from Theorem 3.1, we derive

$$\|e_{\pi_N}(I^{\theta_j}(\bar{p}_{j,n+1}(u)))\|_{\hat{w}^{(0,0)}} \leq CN^{-\rho_j} |I^{\theta_j}(\bar{p}_{j,n+1}(u))|_{\rho_j, \hat{w}^{(0,0)}}. \quad (34)$$

Inserting (33) and (34) into (32) gives

$$\|\bar{e}_{j,N}(u)\|_{\hat{w}^{(0,0)}} - CN^{-\epsilon_{jr}} \sum_{r=1}^n \|\bar{e}_{r,N}(u)\|_{\hat{w}^{(0,0)}} \leq CH_j, \quad (35)$$

in which

$$H_j = N^{-\epsilon_{jr}} |I^{\theta_j}(\bar{p}_{j,r}(u)\bar{v}_r(u))|_{\epsilon_{jr}, \hat{w}^{(0,0)}} + N^{-\rho_j} |I^{\theta_j}(\bar{p}_{j,n+1}(u))|_{\rho_j, \hat{w}^{(0,0)}}.$$

It is straightforward to rewrite (35) in the vector-matrix form

$$G\underline{e} \leq C\underline{H}, \quad (36)$$

where

$$\begin{aligned} \underline{e} &= [\|\bar{e}_{1,N}\|_{\hat{w}^{(0,0)}}, \|\bar{e}_{2,N}\|_{\hat{w}^{(0,0)}}, \dots, \|\bar{e}_{n,N}\|_{\hat{w}^{(0,0)}}]^T, \\ \underline{H} &= [H_1, H_2, \dots, H_n]^T, \end{aligned}$$

and G is a matrix of order n with the entries

$$(G)_{j,r=1}^n = \begin{cases} 1 - CN^{-\epsilon_{jj}}, & r = j, \\ -CN^{-\epsilon_{jr}}, & r \neq j. \end{cases}$$

It follows that, for sufficiently large N , the matrix G converges to the identity matrix. Therefore, the inequality (36) yields

$$\|\bar{e}_{j,N}\|_{\hat{w}^{(0,0)}} \leq CH_j,$$

which proves the desired result. \square

Remark 4.1. *It should be emphasized that D_u^k is not the classical derivative operator; rather, it is the derivative defined in (11) for the transformed space $H_{\hat{w}^{(0,0)}}^k$. Under the assumptions of Theorem 2.1, the solutions $\bar{v}_j(u)$ are analytic in powers of u^n , which implies that $\{\epsilon_{jr}\}_{j=1}^n = \{\rho_j\}_{j=1}^n = \{\infty\}_{j=1}^n$. Therefore, the proposed method is expected to achieve spectral accuracy in this setting. Although the algorithm can also be applied to equations that do not fully satisfy these assumptions, some conclusions may no longer hold. For all the test problems considered (see Section 5), the assumptions of Theorem 2.1 are indeed satisfied.*

5 Numerical examples

In this section, we present numerical solutions for several SFDEs to demonstrate the accuracy and efficiency of the proposed scheme. The section is structured as follows.

- The numerical errors $E(N)$ and CPU time[§] used are computed to evaluate the performance of the suggested method. For all examples, these errors are measured using the $L^2(\Lambda)$ -norm

$$E(N) = \max_{j=1,2,\dots,n} \|e_{j,N}(t)\|, \quad \|e_{j,N}\|^2 \simeq \frac{T}{2} \sum_{k=0}^N \left(e_{j,N}(T/2(x_k^{(0,0)} + 1)) \right)^2 w_k^{(0,0)},$$

where $e_{j,N}(t) = v_j(t) - v_{j,N}(t)$, and $\{(x_k^{(0,0)}, w_k^{(0,0)})\}_{k=0}^N$ denote the Legendre-Gauss quadrature node-weight pairs [36].

[§]We used the `Timing` function in Mathematica to report CPU time.

- To demonstrate the capability of our implementation in handling highly oscillatory solutions of SFDEs, we compare its performance with existing methods from the literature.
- To assess the stability of the proposed approach, we examine its performance for large values of N and for problems defined over an extended integration domain Λ .

All the calculations were executed using Mathematica v13.3, running on an Intel (R) Core (TM) i7-8665U CPU @ 1.90 GHz with 16 GB of RAM.

Example 5.1. Consider the highly oscillatory linear SFDEs

$$\begin{cases} D_C^{\theta_1} v_1(t) = t^{1/2} v_1(t) + v_2(t) + \frac{1}{2} J_0(t^{\frac{5}{4}}) v_3(t) + p_{1,4}(t), \\ D_C^{\theta_2} v_2(t) = v_1(t) + t v_2(t) + 2t^{\frac{3}{2}} v_3(t) + p_{2,4}(t), \\ D_C^{\theta_3} v_3(t) = \sin(2t^{\frac{1}{2}}) v_1(t) + 3v_2(t) + t v_3(t) + p_{3,4}(t), \\ v_1(0) = 0, \quad v_2(0) = v_3(0) = 1, \quad t \in [0, \frac{\pi}{2}], \end{cases}$$

where $J_c(t)$ denotes the Bessel function for the integer c , $\theta_1 = \frac{1}{4}$, $\theta_2 = \frac{1}{2}$, and $\theta_3 = \frac{3}{4}$, and the source functions $p_{j,4}(t)$, $j = 1, 2, 3$, are chosen such that the exact solutions are given by

$$v_1(t) = \sin(70t^{\frac{1}{4}}), \quad v_2(t) = \cos(70t^{\frac{1}{2}}), \quad v_3(t) = \sin(70t^{\frac{3}{4}}) + \cos(12t^{\frac{3}{4}}).$$

This problem exhibits a highly oscillatory solution in which $v_1(t)$ and $v_3(t)$ are not infinitely smooth, and their first derivatives are discontinuous at $t = 0$. Such behavior makes the problem challenging, as its numerical approximation may become unstable for large N . We solve this problem using the proposed method, and the obtained results are presented in Figures 1, 2, and Table 2.

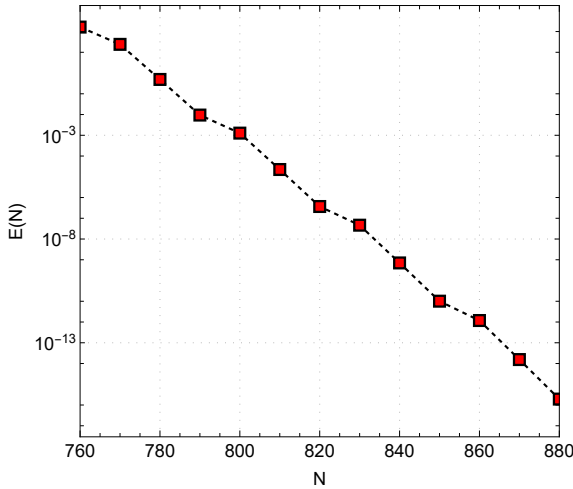


Figure 1: Semi-logarithmic plot of the numerical errors versus N for Example 5.1.

N	CPU Time (s)
110	3.34
220	$1.58 \times 10^{+1}$
440	$6.30 \times 10^{+1}$
880	$5.41 \times 10^{+2}$

Table 2: Elapsed CPU time versus N for Example 5.1.

From Figure 1, we can deduce that the method is converging for $N > 750$, and due to its stability, the error consistently decreases as N increases. Moreover, the semi-log plot of the errors versus N shows a nearly linear trend, indicating an exponential rate of convergence (note that we have $\{\epsilon_{jr}\}_{j=1}^3 = \{\rho_j\}_{j=1}^3 = \{\infty\}_{j=1}^n$ in Theorem 4.1). Figure 2 shows that the approximations exhibit excellent agreement with the exact solution curves, demonstrating the high accuracy of the method. The results validate the method's ability to handle challenging problems with oscillatory behavior and discontinuous derivatives, maintaining both accuracy and stability.

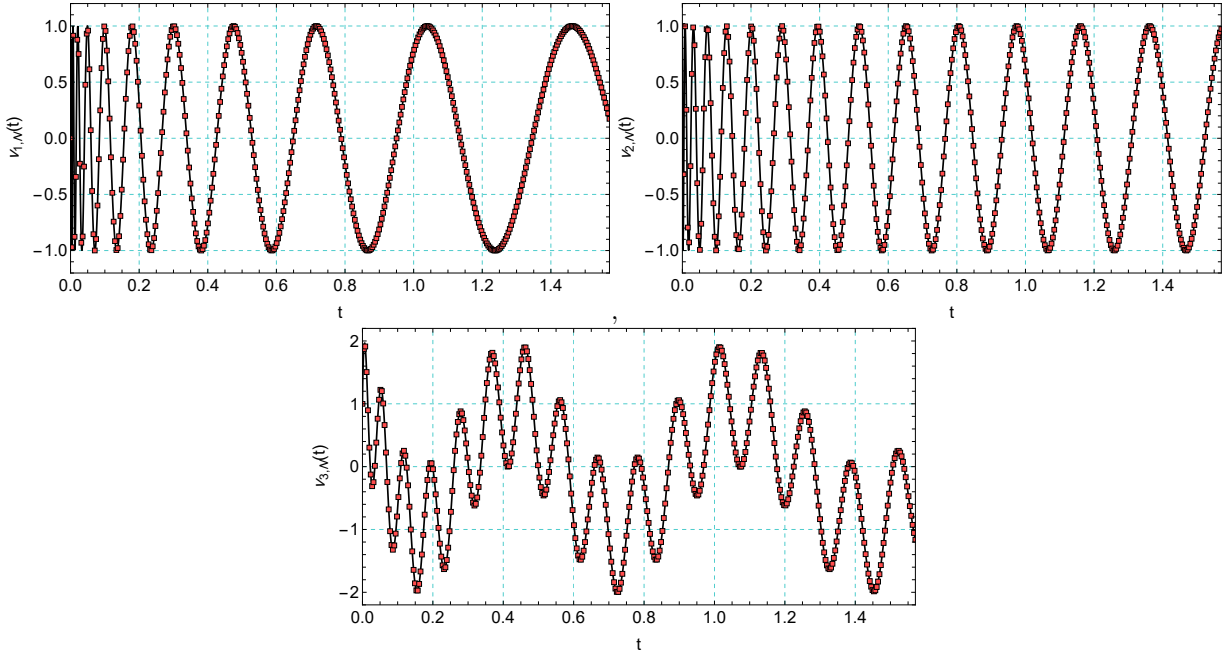


Figure 2: Plots comparing the approximate solutions at $N = 1000$ (red squares) and the exact solutions (solid lines) for Example 5.1.

Example 5.2. Consider the highly oscillatory linear SFDEs

$$\begin{cases} D_C^{\theta_1} v_1(t) = t^{5/2} v_1(t) + v_2(t) + p_{1,3}(t), \\ D_C^{\theta_2} v_2(t) = v_1(t) + \cos(t^{3/2}) v_2(t) + p_{2,3}(t), \\ v_1(0) = 0, \quad v_2(0) = 1, \quad v_2^{(1)}(0) = 1, \quad \Lambda = [0, \frac{3\pi}{2}]. \end{cases}$$

Here we take $\theta_1 = \frac{1}{2}$, $\theta_2 = \frac{3}{2}$, and the functions $p_{j,3}(t)$, $j = 1, 2$, are selected so that the problem admits the following exact solutions

$$v_1(t) = t^{\frac{1}{2}} e^{i80t^{\frac{1}{2}}}, \quad v_2(t) = e^{i10t^{\frac{3}{2}}}.$$

The problem is solved using the proposed method, and the corresponding results are shown in Figure 3, Figure 4, and Table 3.

The forcing functions $p_{j,3}(t)$, $j = 1, 2$, are found to have the following asymptotic behaviors

$$\begin{aligned} p_{1,3}(t) &= -(1.14 \times 10^{-1}) + (9.03 \times 10^1 i) t^{1/2} - (4.25 \times 10^3) t - (1.28 \times 10^5 i) t^{3/2} + \dots, \\ p_{2,3}(t) &= -(1.00 - 1.33 \times 10^1 i) - t^{1/2} + (8.00 \times 10^1 i) t + (2.97 \times 10^3 - 1.00 \times 10^1 i) t^{3/2} + \dots \end{aligned}$$

Consequently, $v_j(s^q)$, and $q_{j,r}(s^q)$ for $q = 2$ are analytic functions and thereby we have $\{\epsilon_{jr}\}_{j=1}^2 = \{\rho_j\}_{j=1}^2 = \{\infty\}_{j=1}^2$ in Theorem 4.1. This establishes the exponential-type convergence of the approximate solutions, as illustrated in Figure 3, while the semi-logarithmic plot of the numerical errors exhibits an almost linear dependence on N . Moreover, Figure 4 shows that the approximate solutions coincide closely with the exact solutions at the selected nodes, confirming the reliability and high-order accuracy of the approximations.

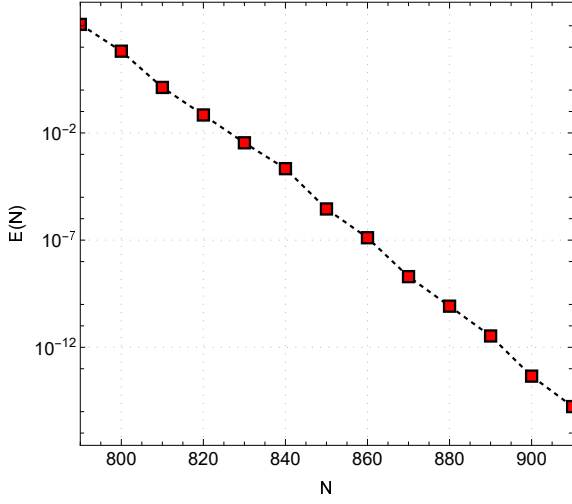


Figure 3: Semi-logarithmic plot of the numerical errors versus N for Example 5.2.

N	CPU Time (s)
125	2.78
250	$1.61 \times 10^{+1}$
500	$5.61 \times 10^{+1}$
1000	$4.32 \times 10^{+2}$

Table 3: Elapsed CPU time versus N for Example 5.2.

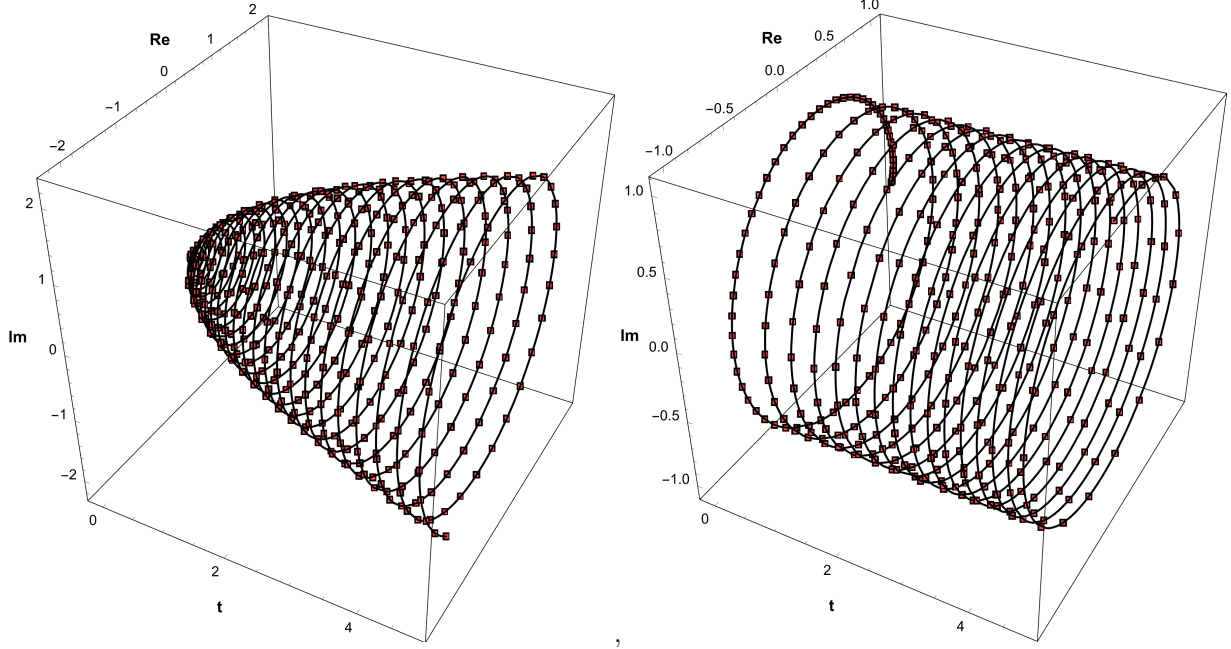


Figure 4: Plots comparing the approximate solutions at $N = 1200$ (red squares) and the exact solutions (solid lines) for Example 5.2.

Example 5.3. Consider the following SFDEs

$$\begin{cases}
 D_C^{\theta_1} v_1(t) = 2tv_1(t) + t^{\frac{1}{3}}v_2(t) + \sin(2t^{\frac{1}{6}})v_3(t) + p_{1,4}(t), \\
 D_C^{\theta_2} v_2(t) = t^{\frac{11}{6}}v_1(t) + t^{\frac{1}{2}}v_2(t) + 5v_3(t) + p_{2,4}(t), \\
 D_C^{\theta_3} v_3(t) = tv_1(t) + v_2(t) + \cos(t^{\frac{2}{3}})v_3(t) + p_{3,4}(t), \\
 v_1(0) = v_2(0) = v_3(0) = 0, \quad \Lambda = [0, 1],
 \end{cases} \quad (37)$$

with the non-smooth solutions

$$v_1(t) = \sin(10t^{\frac{1}{6}}), \quad v_2(t) = t^{\frac{1}{3}}, \quad v_3(t) = t^{\frac{2}{3}} + 5t^{\frac{5}{6}}.$$

Given the exact solutions above, the forcing functions $p_{j,4}(t)$, $j = 1, 2, 3$, are determined so that these solutions satisfy (37).

We solve this problem using our proposed method and the fractional collocation method introduced by Faghieh and Mokhtary [14], and the corresponding semi-logarithmic plots of the errors are presented in Figure 5. Table 4 reports the elapsed CPU times for both methods.

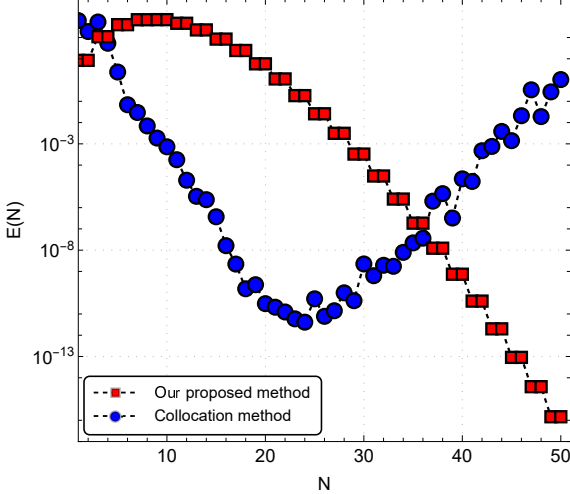


Figure 5: Semi-logarithmic plot of the numerical errors versus N for Example 5.3.

N	CPU Time (s)	
	Proposed method	Collocation method
10	1.09×10^{-1}	6.25×10^{-1}
20	1.41×10^{-1}	1.88
40	2.81×10^{-1}	$2.16 \times 10^{+1}$
80	8.13×10^{-1}	$1.95 \times 10^{+2}$

Table 4: Comparison of elapsed CPU times between our proposed method and the collocation method in [14] for Example 5.3.

In collocation methods, the residual equation is evaluated at a selected set of collocation nodes, leading to a linear system of algebraic equations that, in most cases, has a dense coefficient matrix [14]. Solving such systems can result in reduced accuracy as shown in Figure 5, particularly for oscillatory solutions, where achieving high accuracy often requires large approximation degrees. From Figure 5, we observe that although the collocation method converges more rapidly than our proposed method for small N , the error reaches a lower bound around 10^{-11} , beyond which increasing N no longer improves accuracy. Higher approximation degrees lead to greater accumulation of rounding errors and a more ill-conditioned dense algebraic system (e.g., for $N = 30$, the condition number of the resulting algebraic system is around 10^7). Consequently, for $N \geq 25$, the error grows sharply.

In contrast, the proposed Müntz–Jacobi Galerkin algorithm yields significantly better approximations with considerably shorter CPU times. A regular and steady decrease in the error is observed, demonstrating the advantage of our approach in producing high-accuracy approximations for oscillatory and less-smooth solutions of SFDEs. This advantage partly arises from computing the approximate solutions via recurrence formulas (26), which avoids the formation and solution of large, and potentially ill-conditioned algebraic systems.

In the following, we compare our method with the central part interpolation approach [27] and the hybrid non-polynomial collocation method [17].

Example 5.4. [17, Example 2] Let us consider the linear problem

$$\begin{cases} D_C^\theta v_1(t) = v_2(t), \\ D_C^\theta v_2(t) = -v_1(t) - v_2(t) + t^{\theta+1} + \frac{\pi \csc(\pi\theta)t^{1-\theta}}{\Gamma(-\theta-1)\Gamma(2-\theta)} + \frac{\pi t \csc(\pi\theta)}{\Gamma(-\theta-1)}, \\ v_1(0) = 0, \quad v_2(0) = 0, \quad \Lambda = [0, 1], \end{cases}$$

along with the exact solutions

$$v_1(t) = t^{1+\theta}, \quad v_2(t) = \frac{\pi\theta(\theta+1)\csc(\pi\theta)}{\Gamma(1-\theta)}t.$$

We solve this problem using the proposed scheme for $\theta = \frac{1}{4}, \frac{2}{5}, \frac{1}{2}, \frac{2}{3}$, obtaining exact solutions up to machine precision with approximation degrees $N = 5, 7, 3, 5$, respectively, in a very short CPU time (less than 5.0×10^{-2} (s)). This problem was addressed by Ferrás et al. [17] using a hybrid collocation approach for derivative values $\theta = \frac{1}{4}, \frac{1}{2}, \frac{2}{3}$. This method involves splitting the domain Λ into m subintervals, representing the approximate solutions as a linear combination of non-polynomial functions near the origin, and using polynomials in the remainder of the domain. For the case $\theta = \frac{2}{5}$, Lillemäe et al. [27] proposed a collocation method based on central part interpolation, utilizing continuous piecewise polynomials on a uniform grid. This method involves constructing separate Lagrange interpolation polynomials of degree N for each subinterval, interpolating the solution at $N + 1$ grid points surrounding the subinterval. The numerical results of both methods are summarized in Table 5 for different values of m . As observed, our proposed method achieves higher accuracy compared with both methods presented in [17] and [27].

Table 5: Computed errors for Example 5.4 with m subintervals: hybrid collocation [17] ($N = 4$, $\theta = \frac{1}{4}, \frac{1}{2}, \frac{2}{3}$) and central part interpolation [27] ($N = 4$, $\theta = \frac{2}{5}$).

Hybrid collocation [17]						Central part interpolation [27]	
$\theta = \frac{1}{4}$		$\theta = \frac{1}{2}$		$\theta = \frac{2}{3}$		$\theta = \frac{2}{5}$	
m	max error	m	max error	m	max error	m	max error
15	2.11×10^{-6}	26	1.94×10^{-7}	32	5.53×10^{-8}	64	6.07×10^{-6}
34	1.45×10^{-7}	59	1.27×10^{-8}	71	3.58×10^{-9}	128	2.24×10^{-7}
75	9.43×10^{-9}	128	8.13×10^{-10}	155	2.28×10^{-10}	256	7.61×10^{-9}
166	6.00×10^{-10}	278	5.14×10^{-11}	331	1.44×10^{-11}	512	2.47×10^{-10}

Brugnano et al. [6–8] made a significant contribution to the study of initial value FDEs by developing a class of Runge–Kutta type methods, called fractional Hamiltonian boundary value methods (FHBVMs), along with providing the corresponding Matlab codes available online⁴. In the following two examples, we make a comparison between the Müntz–Jacobi Galerkin method and the approaches presented in [8].

Example 5.5. [8, Problem 1] Given the following linear FDE

$$\begin{cases} D_C^\theta v_1(t) = -v_1(t) + 1, \\ v_1(0) = 10, \quad \Lambda = [0, 10^3], \end{cases}$$

with the exact solution

$$v_1(t) = 9E_{\frac{1}{2}}(-t^{\frac{1}{2}}) + 1,$$

where $E_c(\cdot)$ denotes the one-parameter Mittag-Leffler function, we employ our presented method to solve this equation, and the numerical results are shown in Figure 6 and Table 6.

To assess the performance of the proposed method, we compare it with the approaches introduced by Brugnano et al. [8]. In this work, each approach is addressed by the name of the corresponding Matlab code. A summary of the numerical results obtained with these methods is reported in Table

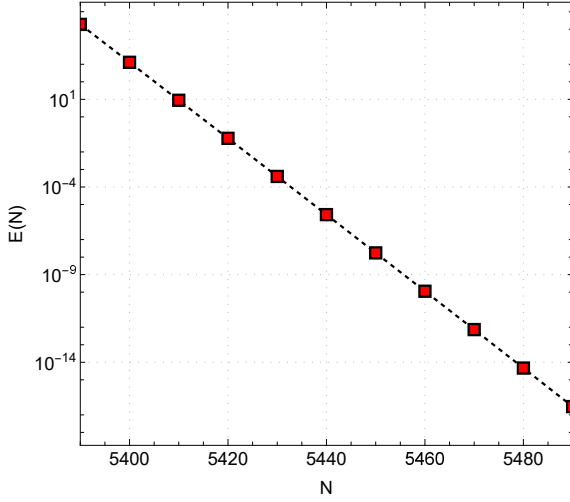


Figure 6: Semi-logarithmic plot of the numerical errors versus N for Example 5.5.

N	CPU Time (s)
685	1.41
1370	6.06
2740	$2.67 \times 10^{+1}$
5480	$9.18 \times 10^{+1}$

Table 6: Elapsed CPU time versus N for Example 5.5.

Method (Code)	Digits of Accuracy	CPU Time (s)
Predictor-corrector (<code>fde12</code>) [18]	6	$5.0 \times 10^{+2}$
Fractional linear multi-step (<code>f1mm2</code>) [19]	10	$7.0 \times 10^{+1}$
Spline collocation (<code>fcoll</code>) [10]	12	0.50
Two-step Spline collocation (<code>tsfcoll</code>) [9]	14	6
FHBVM (<code>fhbvm</code>) [6, 7]	14	5.0×10^{-2}

Table 7: Numerical results obtained through the different methods presented in [8] for Example 5.5.

7. For further details, in particular the plot of the execution time versus accuracy, we refer the reader to [8, Figure 11].

Using the Müntz-Jacobi Galerkin method, we achieve 15 digits of accuracy in less than $8.0 \times 10^{+1}$ (s) of CPU time, which is the highest among all methods reported in Table 7. Although the execution time is shorter than that of the predictor-corrector method (`fde12`), it is longer than the other approaches, while delivering the most accurate results.

It should be noted that the proposed method remains stable and convergent even for problems defined on very long domains, as in this example, or for problems with very highly oscillatory solutions (see Example 5.6). However, achieving small errors in these cases requires very large approximation degrees. For instance, in this example, an error of order 10^{-16} is reached only for $N = 5480$. This inevitably leads to increased computational cost and longer CPU times, indicating that such problems pose greater numerical challenges for the method.

Example 5.6. [8, Problem 4] As the last problem we consider a stiffly oscillatory problem

$$\begin{cases} D_C^{\frac{1}{2}} \mathbf{V}(t) = A \mathbf{V}(t), \\ \mathbf{V}(0) = \mathbf{V}_0, \quad \Lambda = [0, T], \end{cases}$$

[†]<https://people.dimai.unifi.it/brugnano/fhbvm/>

where

$$A = \frac{1}{8} \begin{bmatrix} 41 & 41 & -38 & 40 & -2 \\ -79 & 81 & 2 & 0 & -2 \\ 20 & -60 & 20 & -20 & -8 \\ -22 & 58 & -24 & 20 & -4 \\ 1 & 1 & -2 & -4 & -2 \end{bmatrix}, \quad \mathbf{V}(t) = [v_j(t)]_{j=1}^5, \quad \mathbf{V}_0 = \begin{bmatrix} 1 \\ 2 \\ 3 \\ 4 \\ 5 \end{bmatrix}.$$

The exact solution is given by $\mathbf{V}(t) = E_{\frac{1}{2}}(At^{\frac{1}{2}})\mathbf{V}_0$.

The problem is solved via the suggested method for $T = 2$, and the corresponding results are depicted in Figures 7, 8, and Table 8.

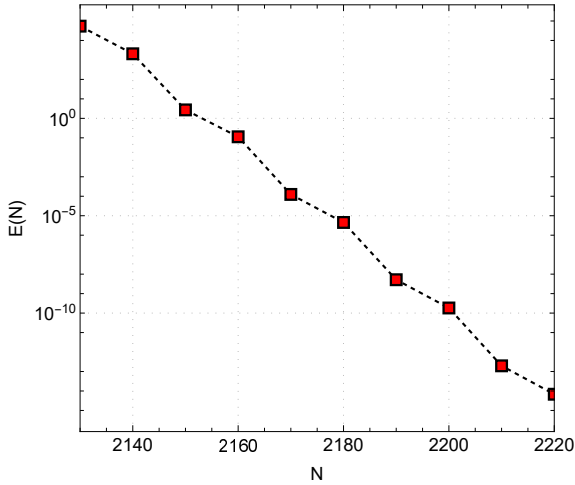


Figure 7: Semi-logarithmic plot of the numerical errors versus N for Example 5.6.

N	CPU Time (s)
280	3.77
560	$1.70 \times 10^{+1}$
1120	$6.84 \times 10^{+1}$
2240	$2.80 \times 10^{+2}$

Table 8: Elapsed CPU time versus N for Example 5.6.

Brugnano et al. [8] addressed this problem using different methods for $T = 20$ (see [8, Figure 14]), and Table 9 summarizes the corresponding results. We were unable to run the example for $T = 20$ via our proposed method on the same computer used for the other experiments, as the longer interval introduces many more oscillations and the problem itself is stiff, exhibiting both fast and slow oscillatory modes. This requires a significantly higher approximation degree to achieve small errors, which in turn, substantially increases the computational cost and necessitates a higher-performance computer. Nevertheless, from the results obtained in both the previous and the current example, it is evident that the FHBVM method is consistently faster than all other methods, while our method achieves higher accuracy. However, the computational cost of our approach becomes considerably larger when solving problems over very long domains with pronounced oscillations. We note that this comparison may not be entirely conclusive, as the other methods were implemented in MATLAB while our method was implemented in Mathematica, so differences in software performance could affect the observed computation times.

6 Conclusion

The main purpose of this paper was to design a high-order spectral method to tackle the highly oscillatory and non-smooth solutions of a class of linear SFDEs. We provided a theorem to identify the conditions under which the solution is highly oscillatory and to extract the regularity properties of the exact solutions. Based on this information, we selected the best choice of basis functions with

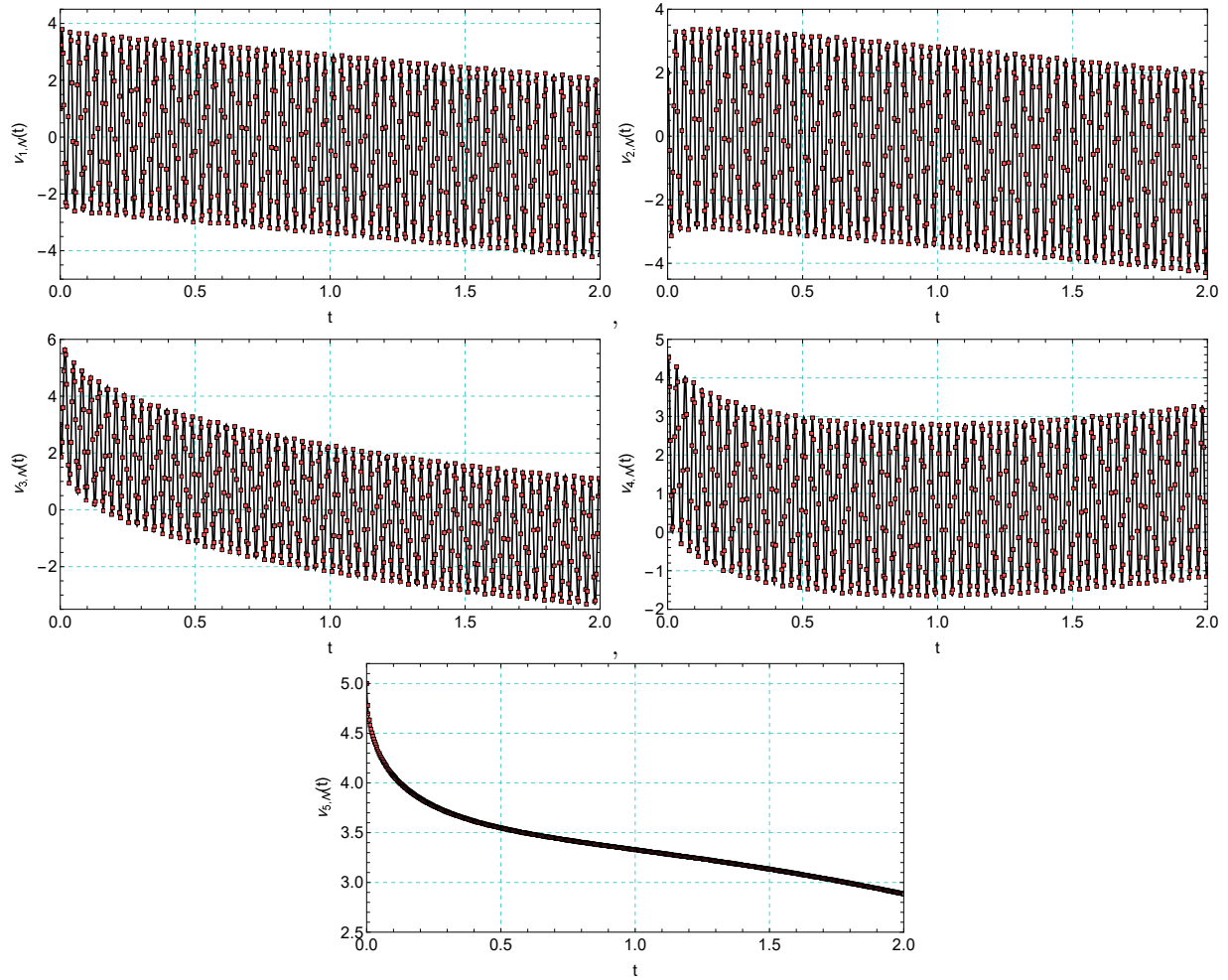


Figure 8: Plots comparing the approximate solutions at $N = 2300$ (red squares) and the exact solutions (solid lines) for Example 5.6.

Method (Code)	Digits of Accuracy	CPU Time (s)
Predictor-corrector (fde12) [18]	3	$2.50 \times 10^{+3}$
Fractional linear multi-step (flmm2) [19]	2	$7.0 \times 10^{+2}$
FHBVM (fhbvm) [6,7]	10	1.5

Table 9: Numerical results obtained through the different methods presented in [8] for Example 5.6.

the same asymptotic behavior as the exact solutions. The Müntz-Jacobi Galerkin method was implemented so that all unknowns were computed through recurrence relations, without the need to solve any potentially ill-conditioned algebraic systems. The choice of basis functions and implementation, together with the provided error analysis, confirmed that the method achieved spectral accuracy under the assumptions of the regularity theorem.

Although an error analysis was provided in this paper, future research will focus on a thorough investigation of the stability properties of the proposed method.

Funding

The research was partially supported by the Research Council KU Leuven (Belgium), through project C16/21/002 (Manifactor: Factor Analysis for Maps into Manifolds) and by the Fund for Scientific Research – Flanders (Belgium), projects G0A9923N (Low rank tensor approximation techniques for up- and downdating of massive online time series clustering) and G0B0123N (Short recurrence relations for rational Krylov and orthogonal rational functions inspired by modified moments).

Acknowledgements

The author would like to thank Marc Van Barel and Raf Vandebril for carefully reading a draft of this paper and for their valuable suggestions.

Declarations

Conflict of interest: The author declares that there is no conflict of interest nor competing interests.

References

- [1] M. H. ATABAKZADEH, M. H. AKRAMI, AND G. H. ERJAEI, *Chebyshev operational matrix method for solving multi-order fractional ordinary differential equations*, Appl. Math. Model., 37 (2013), pp. 8903–8911.
- [2] T. M. ATANACKOVIC, S. PILIPOVIC, B. STANKOVIC, AND D. ZORICA, *Fractional Calculus with Applications in Mechanics: Vibrations and Diffusion Processes*, John Wiley & Sons, 2014.
- [3] D. BALEANU, K. DIETHELM, E. SCALAS, AND J. J. TRUJILLO, *Fractional Calculus: Models and Numerical Methods*, World Scientific, Singapore, 2012.
- [4] A. H. BHRAWY, Y. A. ALHAMED, D. BALEANU, AND A. A. AL-ZAHRANI, *New spectral techniques for systems of fractional differential equations using fractional-order generalized Laguerre orthogonal functions*, Fract. Calc. Appl. Anal., 17 (2014), pp. 1137–1157.
- [5] A. H. BHRAWY AND M. A. ZAKY, *Shifted fractional-order Jacobi orthogonal functions: application to a system of fractional differential equations*, Appl. Math. Model., 40 (2016), pp. 832–845.
- [6] L. BRUGNANO, G. GURIOLI, AND F. IAVERNARO, *Numerical solution of FDE-IVPs by using fractional HBVMs: the fhbvm code*, Numer. Algorithms, 99 (2025), pp. 463–489.
- [7] L. BRUGNANO, G. GURIOLI, F. IAVERNARO, AND M. VIKERPUUR, *Analysis and implementation of collocation methods for fractional differential equations*, J. Sci. Comput., 104 (2025), p. 92.
- [8] ———, *FDE-Testset: comparing Matlab codes for solving fractional differential equations of Caputo type*, Fractal and Fractional, 9 (2025), p. 312.
- [9] A. CARDONE, D. CONTE, AND B. PATERNOSTER, *A Matlab code for fractional differential equations based on two-step spline collocation methods*, in INdAM Workshop on Fractional Differential Equations: Modeling, Discretization, and Numerical Solvers, Springer Nature Singapore, Singapore, 2021, pp. 121–146.
- [10] A. CARDONE, D. CONTE, AND B. PATERNOSTER, *A Matlab implementation of spline collocation methods for fractional differential equations*, in International Conference on Computational Science and Its Applications, Cham, September 2021, Springer International Publishing, pp. 387–401.

- [11] Y. CHEN, X. KE, AND Y. WEI, *Numerical algorithm to solve system of nonlinear fractional differential equations based on wavelets method and the error analysis*, Appl. Math. Comput., 251 (2015), pp. 475–488.
- [12] K. DIETHELM, *The analysis of fractional differential equations*, vol. 2004 of Lecture Notes in Mathematics, Springer-Verlag, Berlin, 2010. An application-oriented exposition using differential operators of Caputo type.
- [13] A. FAGHIH AND P. MOKHTARY, *An efficient formulation of Chebyshev tau method for constant coefficients systems of multi-order FDEs*, J. Sci. Comput., 82 (2020), pp. Paper No. 6, 25.
- [14] ———, *A new fractional collocation method for a system of multi-order fractional differential equations with variable coefficients*, J. Comput. Appl. Math., 383 (2021), pp. Paper No. 113139, 25.
- [15] ———, *A novel Petrov-Galerkin method for a class of linear systems of fractional differential equations*, Appl. Numer. Math., 169 (2021), pp. 396–414.
- [16] ———, *Non-linear system of multi-order fractional differential equations: theoretical analysis and a robust fractional Galerkin implementation*, J. Sci. Comput., 91 (2022), pp. Paper No. 35, 30.
- [17] L. L. FERRÁS, N. J. FORD, M. L. MORGADO, AND M. REBELO, *High-order methods for systems of fractional ordinary differential equations and their application to time-fractional diffusion equations*, Math. Comput. Sci., (2020), pp. 1–17.
- [18] R. GARRAPPA, *On linear stability of predictor-corrector algorithms for fractional differential equations*, Int. J. Comput. Math., 87 (2010), pp. 2281–2290.
- [19] ———, *Trapezoidal methods for fractional differential equations: Theoretical and computational aspects*, Math. Comput. Simul., 110 (2015), pp. 96–112.
- [20] F. GHOLAMI BAHADOR, P. MOKHTARY, AND M. LAKESTANI, *A fractional coupled system for simultaneous image denoising and deblurring*, Comput. Math. Appl., 128 (2022), pp. 285–299.
- [21] ———, *Mixed poisson-gaussian noise reduction using time-space fractional differential equations*, Inf. Sci., 647 (2023), p. 119417.
- [22] R. HERRMANN, *Fractional Calculus: An Introduction for Physicists*, World Scientific, New Jersey, 2011.
- [23] R. HILFER, ed., *Applications of Fractional Calculus in Physics*, World Scientific, Singapore, 2000.
- [24] M. M. KHADER, T. S. EL DANAF, AND A. S. HENDY, *A computational matrix method for solving systems of high order fractional differential equations*, Appl. Math. Model., 37 (2013), pp. 4035–4050.
- [25] M. M. KHADER, N. H. SWEILAM, AND A. M. S. MAHDY, *Two computational algorithms for the numerical solution for system of fractional differential equations*, Arab J. Math. Sci., 21 (2015), pp. 39–52.
- [26] A. A. KILBAS, H. M. SRIVASTAVA, AND J. J. TRUJILLO, *Theory and Applications of Fractional Differential Equations*, vol. 204 of North-Holland Mathematics Studies, Elsevier, Amsterdam, 2006.
- [27] M. LILLEMÄE, A. PEDAS, AND M. VIKERPUUR, *Central part interpolation approach for solving initial value problems of systems of linear fractional differential equations*, Mathematics, 13 (2025), p. 2573.

- [28] R. L. MAGIN, *Fractional Calculus in Bioengineering*, Begell House Publishers, Redding, CA, 2006.
- [29] F. MAINARDI, *Fractional Calculus and Waves in Linear Viscoelasticity*, Imperial College Press, London, 2010.
- [30] M. D. ORTIGUEIRA, *Fractional Calculus for Scientists and Engineers*, vol. 84 of Lecture Notes in Electrical Engineering, Springer, Dordrecht, The Netherlands, 2011.
- [31] A. OUSTALOUP, *La dérivation non entière: théorie, synthèse et applications*, Hermes, Paris, 1995.
- [32] E. PELLEGRINO, L. PEZZA, AND F. PITOLLI, *A collocation method in spline spaces for the solution of linear fractional dynamical systems*, Math. Comput. Simulation, 176 (2020), pp. 266–278.
- [33] I. PETRÁŠ, *Fractional-Order Nonlinear Systems: Modeling, Analysis and Simulation*, Nonlinear Physical Science, Springer, Berlin, Heidelberg, 2011.
- [34] I. PODLUBNY, *Fractional Differential Equations*, Academic Press, San Diego, CA, 1999.
- [35] J. SABATIER, O. P. AGRAWAL, AND J. A. TENREIRO MACHADO, eds., *Advances in Fractional Calculus: Theoretical Developments and Applications in Physics and Engineering*, Springer, Dordrecht, The Netherlands, 2007.
- [36] J. SHEN, T. TANG, AND L.-L. WANG, *Spectral Methods: Algorithms, Analysis and Applications*, vol. 41 of Springer Series in Computational Mathematics, Springer, Berlin, Heidelberg, 2011.
- [37] J. SHEN AND Y. WANG, *Müntz-Galerkin methods and applications to mixed Dirichlet-Neumann boundary value problems*, SIAM J. Sci. Comput., 38 (2016), pp. A2357–A2381.
- [38] V. TARASOV, *Fractional Dynamics: Applications of Fractional Calculus to Dynamics of Particles, Fields and Media*, Springer-Verlag Berlin Heidelberg, 2010.
- [39] V. V. UCHAIKIN, *Fractional Derivatives for Physicists and Engineers: Volume I, Background and Theory*, Nonlinear Physical Science, Springer and Higher Education Press, Berlin and Beijing, 2013.
- [40] J. WANG, T. Z. XU, Y. Q. WEI, AND J. Q. XIE, *Numerical solutions for systems of fractional order differential equations with Bernoulli wavelets*, Int. J. Comput. Math., 96 (2019), pp. 317–336.
- [41] Q. YANG, D. CHEN, T. ZHAO, AND Y. CHEN, *Fractional calculus in image processing: a review*, Fract. Calc. Appl. Anal., 19 (2016), pp. 1222–1249.
- [42] M. A. ZAKY, *An accurate spectral collocation method for nonlinear systems of fractional differential equations and related integral equations with nonsmooth solutions*, Appl. Numer. Math., 154 (2020), pp. 205–222.